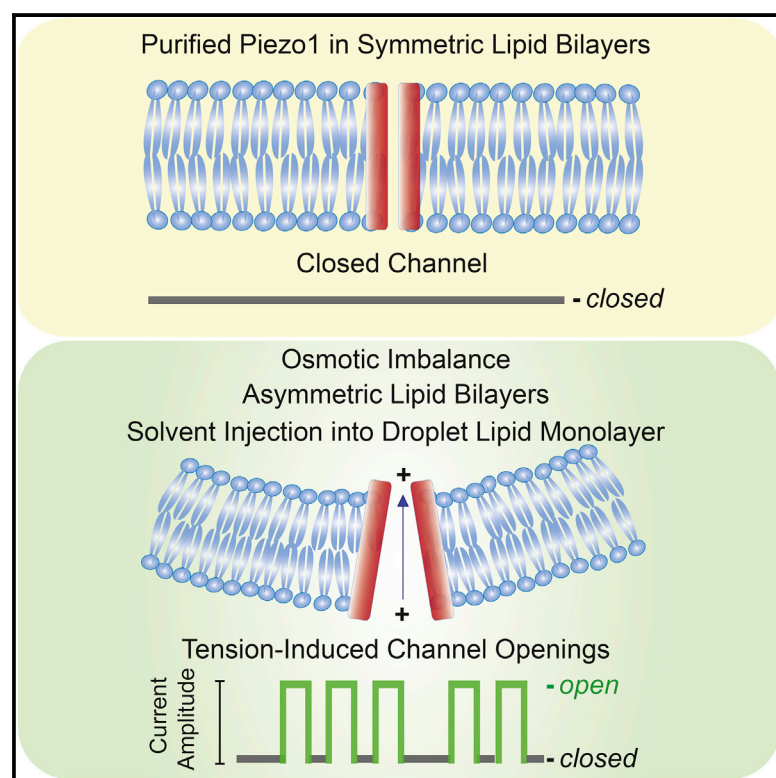# Cell Reports

Piezo1 Channels Are Inherently Mechanosensitive

Graphical Abstract

Authors
Ruhma Syeda, Maria N. Florendo, Charles D. Cox, Jennifer M. Kefauver, Jose S. Santos, Boris Martinac, Ardem Patapoutian

Correspondence
ruhma@scripps.edu

In Brief
Piezo proteins transduce physical forces and are activated by mechanical indentation and stretching of cell membranes. By reconstituting these channels in lipid bilayers, Syeda et al. show that Piezo1 channels are stimulated in the absence of other cellular components via a variety of methods, including osmotic imbalance and membrane perturbation.

Highlights

- Purified wild-type and mutant Piezo1 channels are active in lipid bilayers

- Piezo1 and MscS, but not KcsA, are active in bilayers with osmotic gradient

- Piezo1 and MscS, but not KcsA, respond to perturbations in membrane tension

- Piezo1 is activated in the absence of other cellular components

CrossMark

CellPress

Report

Piezo1 Channels Are Inherently Mechanosensitive

Ruhma Syeda,[1,6,*] Maria N. Florendo,[1] Charles D. Cox,[2] Jennifer M. Kefauver,[1] Jose S. Santos,[3,5] Boris Martinac,[2,4] and Ardem Patapoutian[1]

[1]Howard Hughes Medical Institute, Molecular and Cellular Neuroscience, Dorris Neuroscience Center, The Scripps Research Institute, La Jolla, CA 92037, USA
[2]Victor Chang Cardiac Research Institute, Lowy Packer Building, 405 Liverpool Street, Darlinghurst, NSW 2010, Australia
[3]Section of Neurobiology, Division of Biological Sciences, University of California, San Diego, La Jolla, CA 92093, USA
[4]St Vincent's Clinical School, University of New South Wales, Darlinghurst, NSW 2010, Australia
[5]Present address: Dart NeuroScience, 12278 Scripps Summit Drive, San Diego, CA 92131, USA
[6]Lead Contact
*Correspondence: ruhma@scripps.edu
http://dx.doi.org/10.1016/j.celrep.2016.10.033

SUMMARY

The conversion of mechanical force to chemical signals is critical for many biological processes, including the senses of touch, pain, and hearing. Mechanosensitive ion channels play a key role in sensing the mechanical stimuli experienced by various cell types and are present in organisms from bacteria to mammals. Bacterial mechanosensitive channels are characterized thoroughly, but less is known about their counterparts in vertebrates. Piezos have been recently established as ion channels required for mechanotransduction in disparate cell types in vitro and in vivo. Overexpression of Piezos in heterologous cells gives rise to large mechanically activated currents; however, it is unclear whether Piezos are inherently mechanosensitive or rely on alternate cellular components to sense mechanical stimuli. Here, we show that mechanical perturbations of the lipid bilayer alone are sufficient to activate Piezo channels, illustrating their innate ability as molecular force transducers.

INTRODUCTION

Hudspeth and colleagues established in the 1970s that hearing is enabled by direct activation of mechanosensitive (MS) ion channels (Corey and Hudspeth, 1979). Since then, a role of MS channels has been established in a variety of cell types, including touch neurons, pain neurons, muscle cells, endothelial cells of blood vessels, and red blood cells, to name a few (Chalfie, 2009; Guharay and Sachs, 1984; Nilius and Honoré, 2012; Ranade et al., 2015). However, the molecular identity of these MS channels has remained elusive. To define an ion channel as a physiologically relevant mechanosensor, various criteria have to be met (Arnadóttir and Chalfie, 2010; Ranade et al., 2015): (1) the gene encoding the mechanosensitive protein must be expressed in mechanosensitive cells, (2) deletion of the gene should abolish mechanosensitivity of the cells while leaving other cellular functions intact, (3) the candidate

mechanosensitive protein should contain a pore-forming subunit for rapid ion conduction, and (4) mutations of amino acids in critical domains should alter the pore properties of the MS currents.

Very few ion channels satisfy all these criteria. Even in those rare cases, it is still unknown whether these channels are inherently mechanosensitive or depend on various cellular components to sense mechanical force. Cellular components that could be required for gating MS channels include auxiliary subunits, extracellular/intracellular tether proteins, specialized lipid domains such as rafts, or small molecules that are released during mechanical stimulation (Anishkin et al., 2014; Gillespie and Walker, 2001; Teng et al., 2015; Zhang et al., 2015). For example, Drosophila mechanically activated channel NOMPC (no mechanoreceptor potential C) has been recently shown to require cytoskeleton connection to confer mechanosensitivity (Zhang et al., 2015). Therefore, the ultimate evidence that an ion channel is inherently MS is to demonstrate its mechanosensitivity in a cell-free environment (Berrier et al., 2013; Brohawn et al., 2014b; Najem et al., 2015; Sukharev et al., 1994). This force transmission directly from lipids to proteins is termed the "force from lipids" concept (Anishkin et al., 2014; Martinac et al., 1990; Teng et al., 2015).

Based on these criteria, bacterial MscS and MscL and mammalian TRAAK and TREK channels are classified as mechanosensitive ion channels. Both MscS and MscL respond to extracellular osmotic challenges to prevent cell lysis (Booth, 2014; Martinac et al., 2014). In contrast the physiological role of TRAAK in mechanotransduction is not completely understood, but it is widely expressed in neurons and is involved in mechanical and thermal nociception in mice (Noël et al., 2009). Various studies in cellular and cell-free environments have established MscS, MscL, TRAAK, and TREK to be inherently mechanosensitive channels (Bass et al., 2002; Battle et al., 2009; Berrier et al., 2013; Brohawn et al., 2014a, 2014b; Dong et al., 2015; Perozo et al., 2002).

In vertebrates, cation-selective Piezo channels are required for mechanotransduction in a number of biological processes (Ranade et al., 2015; Woo et al., 2015) and are necessary and sufficient for the mechanosensitivity of various cells (Coste et al., 2010, 2012). Heterologous expression of Piezos in cells exhibit large mechanically activated currents, and recent reports show
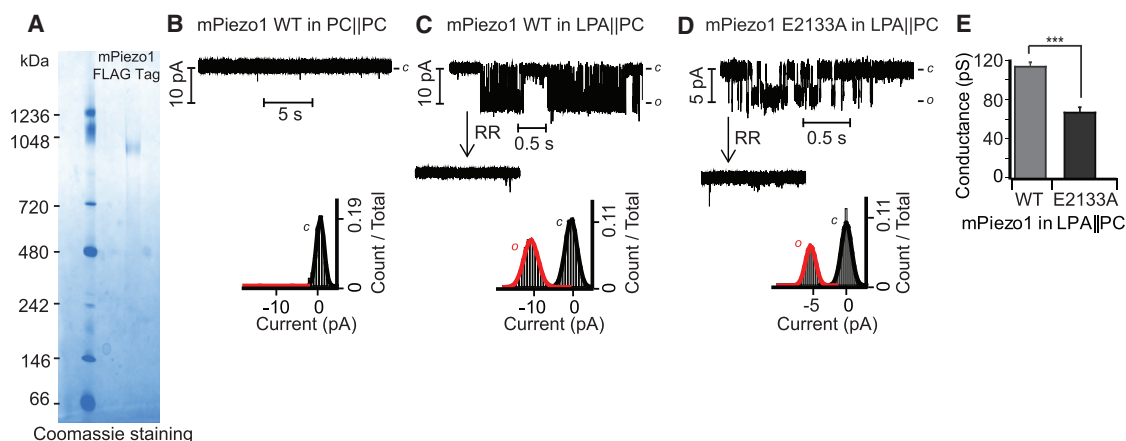
Figure 1. Reconstitution of Piezo1 in Droplet Lipid Bilayers

(A) Purified Piezo1-FLAG separated on Bis-Tris native gel and visualized by Coomassie staining (representative gel from n = 5).

(B–D) Single-channel current recordings in 500 mM KCl, V = −100 mV, and the all-point histograms of purified Piezo1-WT (B and C) and Piezo1-E2133A mutant (D). Channel openings are downward deflections where c represents closed and o represents open. The insets below show the channel block upon RR injection (40 μM final).

(E) Single-channel conductance comparison of Piezo1-WT versus Piezo1-E2133A in LPA||PC lipid bilayers under similar conditions (500 mM KCl, 10 mM HEPES [pH 7.4] at V = −100 mV). The two groups in question are significantly different as determined by two-tailed unpaired t test: ***p < 0.001. Error bars represent SEM. See also Table S1.

that Piezo1 responds to lateral membrane tension in cellular membranes (Coste et al., 2012; Cox et al., 2016; Lewis and Grandl, 2015; Ranade et al., 2015). Indeed, the roles of various cellular components that modulate Piezo channel activity are also emerging (Anishkin et al., 2014). For example, overexpressing a pathogenic mutant of Polycystin-2 (Peyronnet et al., 2013) and depletion of second messenger phosphoinositides (PIP or PIP2) inhibits mechanically activated currents in Piezo-expressing cells (Borbiro et al., 2015). Also, the integral membrane protein STOML3 strongly potentiates Piezo1 and Piezo2 responses to mechanical stimuli (Poole et al., 2014). Furthermore, Piezo1 sensitivity to mechanical indentation is dynamically modified by disruption of the cytoskeleton (Gottlieb et al., 2012) and cytoskeletal element filamin A (Retailleau et al., 2015). Although Piezos satisfy all the criteria required to be MS channels (Ranade et al., 2015), whether the channel is inherently mechanosensitive or whether it requires cellular components to sense mechanical forces is still unknown.

We had shown that purified GST (glutathione S-transferase)-fused Piezo1 reconstituted in asymmetric droplet bilayers (1,2-diphytanoyl-sn-glycero-3-phosphocholine [DPhPC] doped with 1,2-dioleoyl-sn-glycero-3-phosphatidic acid [DOPA] on one monolayer) gave rise to constitutive Piezo1-dependent activity (Coste et al., 2012). We also showed that Piezo1 channel activity was not observed in symmetric DPhPC bilayers but that the application of agonist Yoda1 produced channel activity (Syeda et al., 2015). These experiments suggest that membrane properties play an important role in Piezo1 gating, but they do not directly address whether Piezo1 is inherently mechanosensitive. The chemical activation of Piezo1 in symmetric bilayers raises the possibility of using mechanical forces on symmetrical bilayers to probe whether Piezo1 is mechanosensitive in a cell-free system. Here, we use various manipulations of the droplet-bilayer
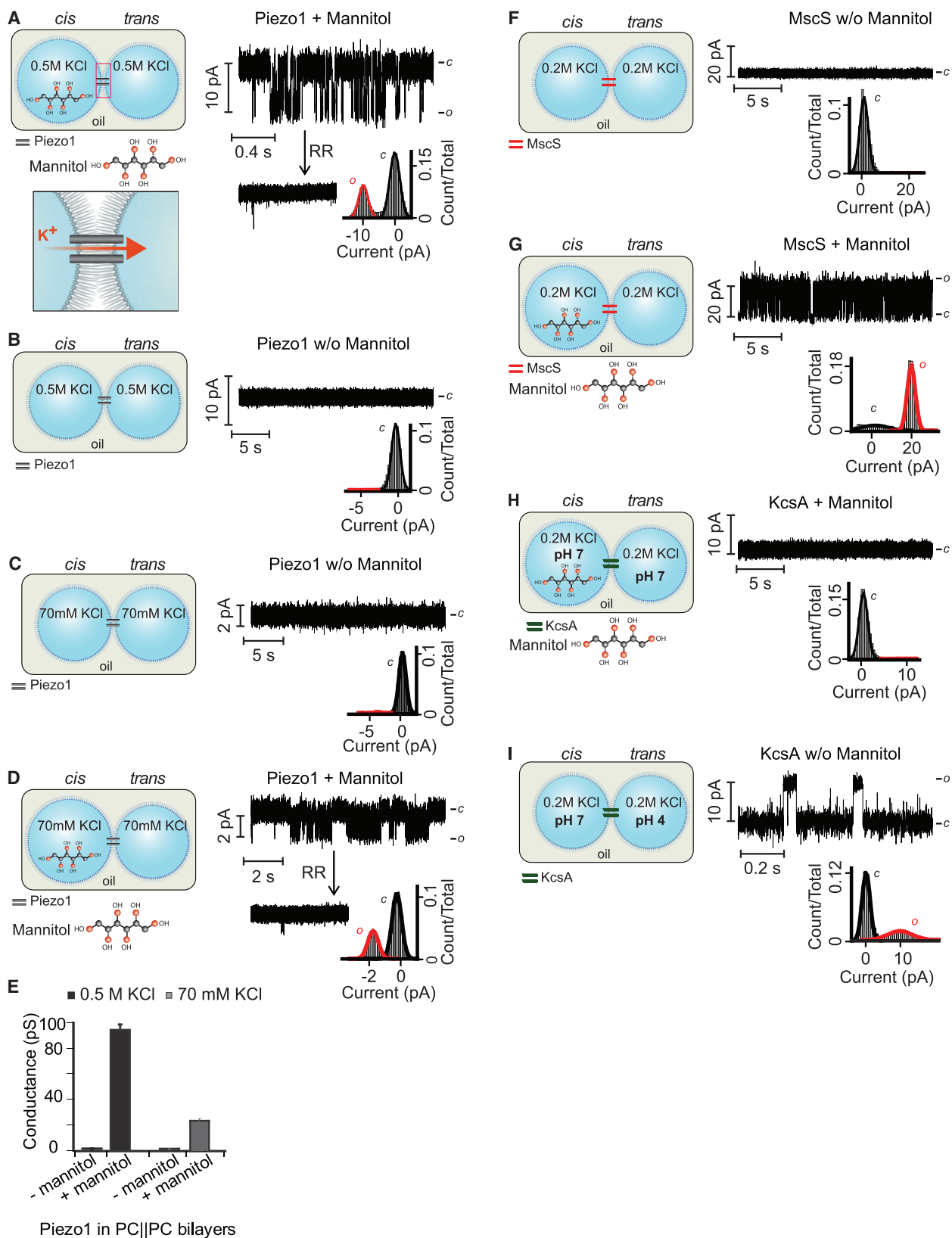
system to provide evidence that Piezo1 directly senses mechanical forces within the membrane.

RESULTS AND DISCUSSION

Evidence that Currents Recorded in Droplet Bilayers Are Derived from Piezo1 Ion Channels

Previously, we used a GST tag to purify Piezo1 ion channels (Coste et al., 2012). Recently, cryo-electron microscopy studies showed that Piezo1 forms a trimer (Ge et al., 2015). This study also showed that GST-tagged Piezo1 can form an artificial dimer of Piezo1 trimers, in addition to a trimer (Ge et al., 2015). To avoid GST-induced dimerization, we used a Piezo1-FLAG construct for overexpression in HEK293T cells, followed by affinity-tag purification (Ge et al., 2015). The identity and homogeneity of the purified protein was assayed by Coomassie blue staining of a native gel (Figure 1A). A single prominent protein band with a molecular weight of ~900 kDa was detected, consistent with trimeric Piezo1 (Figure 1A) (Ge et al., 2015). This purified Piezo1 sample was reconstituted into droplet lipid bilayers for subsequent investigation of its mechanosensitivity.

The FLAG-tagged Piezo1 behaved similarly to the GST fused protein described earlier: Piezo1 activity was not observed when reconstituted in symmetrical DPhPC (phosphatidylcholine||phosphatidylcholine; PC||PC) bilayers (n = 19; Figure 1B) (Coste et al., 2012; Syeda et al., 2015). However, when PC bilayers were doped with lysophosphatidic acid (LPA) on the *cis* monolayer, discrete ruthenium-red (RR)-sensitive channel activity was detected (Figure 1C). RR blocked the currents exclusively from the *trans* droplet; hence, the channels are oriented so that the *cis* droplet represents the intracellular side of the protein (Coste et al., 2012). The calculated single-channel conductance (γ) of Piezo1-FLAG in asymmetric LPA||PC bilayers

was 114 ± 4 pS in 500 mM KCl (n = 6; Table S1). We also calculated the γ of Piezo1-FLAG in DOPA||PC bilayers (γ = 117 ± 5 pS in 500 mM KCl; n = 4; data not shown). Both of these conductance values are in agreement with what we previously calculated for Piezo1-GST-fused protein in asymmetric DOPA||PC bilayers (γ = 118 ± 15 pS; 500 mM KCl, n = 6) (Coste et al., 2012). Furthermore, when similar ionic conditions are compared, the conductance of Piezo1 in cells and droplet lipid bilayers are in agreement (Ranade et al., 2015). Thus, the identity of the tag or a specific asymmetric lipid composition did not change Piezo1 functional properties.

A striking feature of Piezo1 activity in whole-cell recordings is rapid inactivation. However, the recordings from lipid bilayers did not recapitulate such Piezo1 kinetics. This may suggest that specific partners or cellular structures are necessary for Piezo1 inactivation. To quell any remaining concerns that we are recording ionic currents from Piezo1 in bilayers, we assayed the activity of Piezo1 mutant (E2133A) that exhibits reduced γ (~50% of wild-type [WT]) in the cellular assay. The Piezo1 E2133A exhibited a γ of 67 ± 5 pS in LPA||PC bilayers (n = 7) compared to WT Piezo1, γ = 114 ± 4 pS (500 mM KCl; Figures 1D and 1E; Table S1) (Coste et al., 2015). Thus, the electrical activity recorded in droplet lipid bilayers arose from Piezo1 channels.

Activation of Piezo1 upon Stimulation by an Osmotic Gradient

Next, we asked whether reconstituted Piezo1 could be acutely activated by mechanical stimuli. We tested the effect of osmotic stress generated by an osmolyte (mannitol) gradient by supplementing the *cis* droplet with 500 mM mannitol. Under these osmotic stress conditions, single or multiple channels sensitive to RR were observed (n = 10) (Figure 2A; Table S1). Piezo1 exhibited a γ = of 97 ± 4 pS, and open probability (P_o) = 0.5 ± 0.06. Importantly, no Piezo1 channel activity was observed in the presence of mannitol in both droplets or in its absence (n = 9) (Figure 2B). Lipid bilayers are permeable to water. Diffusion of water across the membrane would cause monolayer stretch in one droplet, as well as changes in ionic strength. One mechanistic possibility is that Piezo1 responds to decreased local ionic strength as a consequence of water movement across the membrane, similar to what was observed for volume-regulated anion channels (Syeda et al., 2016). We ruled out that the ionic strength is the cause of Piezo1 activation by recording channel activity in the presence of a reduced ionic concentration (symmetrical 70 mM KCl). Discrete single or multiple channels (n = 7; Table S1) were observed under an osmotic gradient in 70 mM KCl, but no channel activity was observed in the absence of osmotic stress (n = 7) (Figures 2C and 2D). As expected, γ was

reduced in these ionic conditions (24 ± 2 pS), but the P_o was unaffected (0.45 ± 0.08) when compared to 500 mM KCl. These data show that Piezo1 is gated in response to osmotic stress (Figure 2E).

To validate our osmotic stress assay, we examined the activity of other ion channels to serve as positive and negative controls. We tested the well-characterized bacterial mechanosensitive channel MscS. Purified MscS was reconstituted into PC||PC bilayers (200 mM KCl), and the activity was recorded in the presence and absence of 500 mM mannitol (Figures 2F and 2G). In the presence of mannitol, distinct MscS single or multiple channels (n = 6; Table S1) were observed with a γ of 630 ± 30 pS; no activity was observed without osmotic stress (n = 4). The MscS activity induced is "flickery" in nature, in accordance with previous reports in pure lipid bilayers (Ridone et al., 2015), and did not display noticeable inactivation (Cox et al., 2013).

As a negative control, we used the bacterial K^+ channel KcsA (a non-mechano-activated channel) to demonstrate that not every channel reconstituted in droplet bilayers is active under osmotic stress. Indeed, KcsA is not activated by osmotic stimulus while the intracellular side faces pH = 7.0 (n = 8) (Figures 2H and S1). Whereas discrete channel activity exhibiting γ = 114 ± 7 pS in 200 mM KCl was observed when pH = 4.0 is applied, a relevant KcsA-activating stimulus (LeMasurier et al., 2001) (n = 7; Figures 2I and S1; Table S1).

Activation of Piezo1 by Solvent Injection Assay

To complement the osmotic stress data, we tested whether Piezo1 was activated following direct expansion of one droplet monolayer. To achieve this, we injected 30 nL of solvent (500 mM KCl) into the *cis* droplet, which resulted in an area increase of ~15%–30%. The differential droplet area will induce changes in the bilayer tension profile (Supplemental Information). We first tested the effect of injection on PC||PC lipid bilayers and show that the characteristics of the bilayers were maintained after injection (n = 10) (Figures 3A and 3B). Similar injection protocols repeated in the presence of Piezo1 (Figure 3C) resulted in single- or multiple-channel activity with the expected γ = 98 ± 3 pS in 500 mM KCl (n = 8; Figures 3D and 3E; Table S1). As a validation for this assay, we repeated the injection protocols with reconstituted MscS and KcsA. MscS displayed discrete channel openings after solvent injection and exhibited a γ of 630 ± 40 pS in 200 mM KCl (n = 5; Figures 3F and 3G; Table S1). No activity was observed for KcsA (n = 6; Figures 3H and 3I). How much tension is being applied to the membrane in the solvent injection assay? Measurements derived from confocal images estimated the bilayer tension to be 3.4 ± 0.8 mN/m (n = 4), with >75% coming from the *cis* monolayer (Figures 3 and S2). Interestingly, this is in close agreement with

---

Figure 2. Activation of Purified Piezo1 by Osmotic Stress Stimulation

(A–D) Experimental illustrations of droplets with and without an osmotic gradient in the presence of either 500 mM KCl or 70 mM KCl and the single-channel recordings of Piezo1 in PC||PC bilayers at V = −100 mV. c, closed; o, open.

(E) Single-channel conductance comparison of Piezo1 for the indicated experimental conditions. The two groups in question are significantly different as determined by two-tailed unpaired t test: p < 0.001. Error bars represent SEM.

(F and G) Single-channel recordings of MscS in PC||PC bilayers in the absence and presence of osmotic stress with 200 mM KCl at V = 30 mV.

(H and I) Single-channel recordings of KcsA in the indicated pH solutions in the absence and presence of osmotic stress with 200 mM KCl at V = +100 mV.
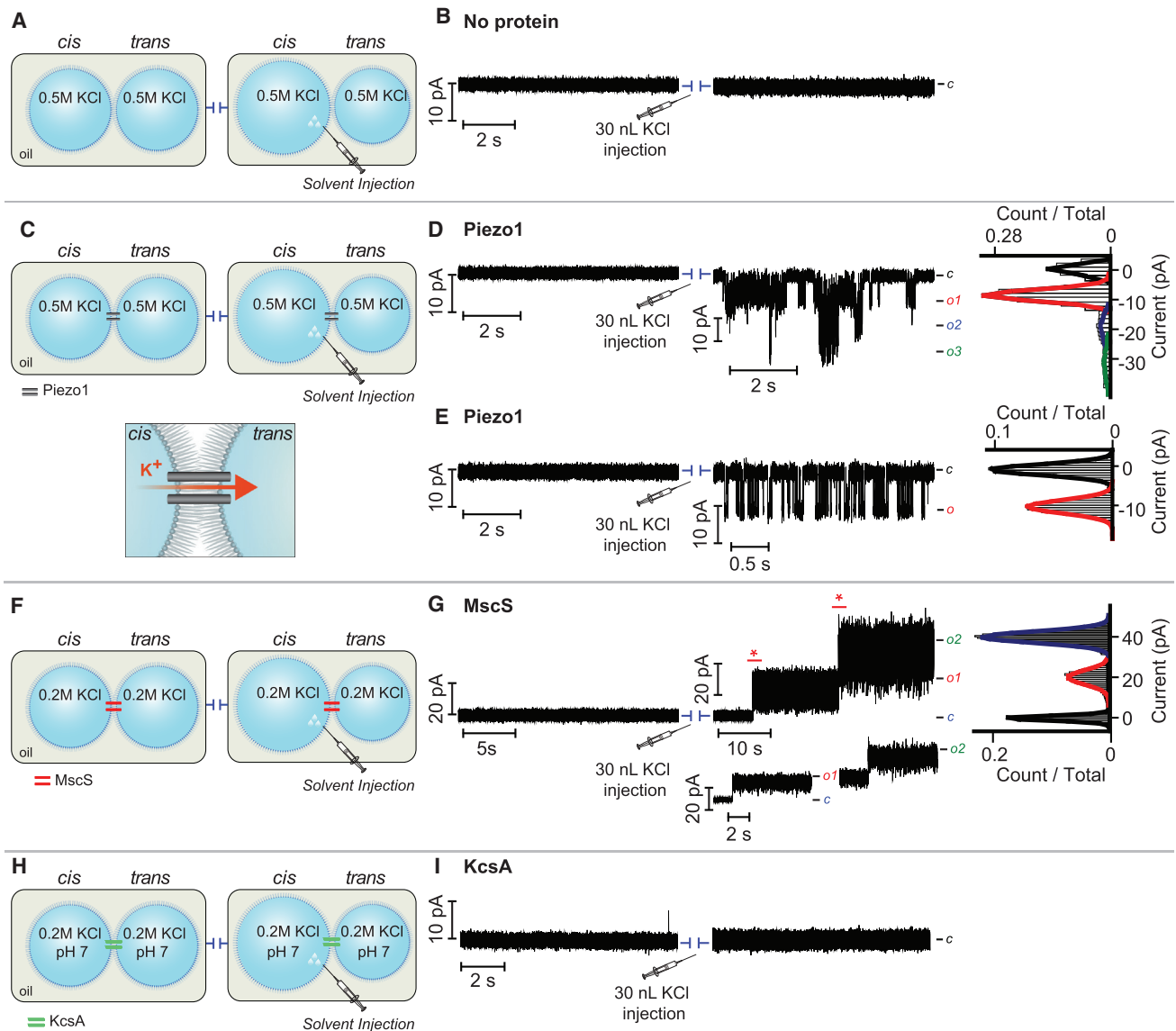
See also Figure S1 and Table S1.

Figure 3. Activation of Piezo1 by Solvent Injection in the Lipid Monolayer
(A and B) Illustration of the solvent injection assay and electrical recordings in the absence of protein before and after the injection protocols. *c*, closed.
(C–I) Illustration of the solvent injection assay and examples of electrical recordings in the presence of (C–E) Piezo1 in 500 mM KCl, V = −100 mV; (F and G) MscS in 200 mM KCl, V = 30 mV; and (H and I) KcsA in 200 mM KCl, V = 100 mV. *o*, open.
See also Figure S2, Table S1, and Supplemental Experimental Procedures.

previously reported values for the tension threshold of both MscS (3–4 mN/m) (Nomura et al., 2012, 2015) and Piezo1 activation (∼2–3 mN/m) (Cox et al., 2016; Lewis and Grandl, 2015).

In summary, we establish that Piezo1 mechanosensitivity in droplet lipid bilayers follows the force-from-lipids paradigm by responding to mechanical forces in the lipid bilayer without the requirement for any other cellular components (Kung, 2005; Martinac et al., 1990; Teng et al., 2015). The methods used here to study Piezo1 activation (membrane asymmetry, osmotic stress, and solvent injection) are quite distinct in nature. However, they evoke asymmetric changes in the transbilayer pressure profile. Our data provide evidence that Piezo1 detects forces—in

particular, tension—imparted by the lipid bilayer alone. This is consistent with a recent report that Piezo1 responds to lateral membrane tension in cells (Lewis and Grandl, 2015). Furthermore, mechanosensitivity of Piezo1 is also preserved in membrane blebs, which are largely free of cytoskeleton (Cox et al., 2016). However, our data do not argue that other factors are not involved in modulating Piezo mechanosensitivity. For example, the cytoskeleton and associated proteins, such as STOML3, regulate the mechanosensitivity of Piezo1 (Borbiro et al., 2015; Gottlieb et al., 2012; Poole et al., 2014). Regardless, our studies establish that, like the bacterial MS channels, the mechanosensitivity of Piezo1 is inherent, and no other proteins or

second-messenger signals are required for the baseline mecha-nosensitivity of Piezo1.

EXPERIMENTAL PROCEDURES

Mouse Piezo1-FLAG Tag Purification

The mouse Piezo1-FLAG construct and mouse Piezo1-FLAG E2133A mutant were both assembled using the QuikChange XL Site-Directed Mutagenesis Kit from Agilent Technologies. Using designed primers and Piezo1-ires-pcDNA3.1 as a template, the FLAG sequence was inserted as a C-terminal fusion to Piezo1, creating the Piezo1-FLAG construct. The Piezo1-FLAG E2133A mutant was assembled by changing the amino acid at position E2133 of the Piezo1-cFLAG-ires-pcDNA3.1 construct from "E" to "A" (codons GAG to GCG). The plasmids were transformed to XL10-Gold competent cells. Positive clones were screened and verified by full-length sequencing. HEK293 cells were used for the production of protein because of its easily transfectable nature and its ability to efficiently produce proteins. We specifically used the HEK293T cell line, which is derived from HEK293s and includes a simian virus 40 (SV40) T antigen for increased protein production of vectors. 48 hr after transfection, HEK293T cells were collected from four to six confluent 500-cm^2 dishes and incubated in a homogenizing buffer containing 20 mM Tris-HCl (pH 8.0), 50 mM NaCl, 1 mM EGTA, 5 mM EDTA, 20 μg pepstatin, and a protease inhibitor cocktail for 15 min. This cell suspension was homogenized using a glass pulverizer and forced through a 27.5G needle ten times. After homogenization, the mixture was centrifuged at 4°C for 15 min at 3,500 rpm. The supernatant was collected and centrifuged at 4°C for 45 min at 53,000 rpm. A second centrifugation step was performed to wash the membrane pellet using the same conditions as the previous spin.

The protein was extracted from the membrane pellet by using the glass pulverizer and extraction buffer: 20 mM Tris-HCl (pH 8.0), 150 mM NaCl, 1 mM EGTA, 1% CHAPS, 0.5% PC, iodoacetamide (4 mg/mL), and a cocktail of protease inhibitors. The protein was purified by ANTI-FLAG M2 Affinity Gel (Sigma-Aldrich, catalog #A2220). The resin was prepared in a batch mode, as per the user manual and technical bulletin. The extracted protein was incubated with the resin overnight, with rotation at 4°C. The protein was eluted with 3×FLAG peptide (100 μg/mL) in the elution buffer: 150 mM NaCl, 50 mM Tris-HCl (pH 8.0), 0.6% CHAPS, 0.1% PC, and a protease inhibitor cocktail. Two thirds of this sample was used for proteoliposome, while the rest was analyzed using a native gel. Similar purification protocols were performed for the mutant E2133A.

NativePAGE Novex Bis-Tris Gel

The eluted protein samples were analyzed using a non-denaturing 3%–12% NativePAGE Novex Bis-Tris gel electrophoresis in accordance with the user manual (Invitrogen). Each sample was mixed with NativePAGE Sample Buffer and NativePAGE 5% G-250 Sample Additive and then run on a gel at 150 V for 2 hr. After electrophoresis, the native gel was visualized using Coomassie G-250 staining.

MscS Purification

MscS protein containing a C-terminally linked 6xHis-tag was expressed in *E. coli* and purified using immobilized-metal affinity chromatography similar to a previously reported protocol (Vásquez et al., 2007). Briefly, cells were disrupted using a French press (French Cellular Press, Thermo Scientific), and membranes were solubilized overnight at 4°C in a PBS-based buffer (pH 7.5) containing 8 mM DDM, 10% glycerol, and PMSF. Solubilized supernatant was incubated with cobalt resin (Talon, Clontech) for 3 hr at 4°C subsequent to a pre-wash with PBS (pH 7.5) supplemented with 1 mM DDM (eight times the resin volume). The protein was finally eluted with 300 mM imidazole, 1 mM DDM, and 10% glycerol in PBS buffer (pH 6). Protein was desalted using buffer exchange and the use of an Amicon filter (Millipore, Amicon Ultra-15 Centrifugal Filter Device).

Formation of Proteoliposomes

Proteoliposomes were formed by incorporating purified Piezo1 (WT or E2133A), MscS, or KcsA in asolectin liposomes. First, asolectin liposomes (5 mg/mL) were prepared by resuspending dried asolectin lipids (L-α-phosphatidylcholine, Avanti Polar Lipids, catalog #840054) in 200 mM KCl, 10 mM HEPES (pH 7.2). The liposomes were then extruded through a 0.1-mm filter (Whatman Nucleopore Track-Etch membrane). Asolectin liposomes (400 μL at 5 mg/mL) were semi-permeabilized for 1 hr at room temperature with rotation, by adding 18 μL DDM (200 mM stock). Purified proteins (5–10 μL) were added in the semi-permeabilized liposomes (5 mg/mL) and incubated with rotation at room temperature for 1 hr. This proteoliposome sample (protein mass:lipid mass ratio of ~1:400) was then subjected to a Slide-A-Lyzer dialysis cassette with a molecular cutoff weight of 3.5 KDa (Thermo Scientific, product #66330) to eliminate excess CHAPS detergent and FLAG peptide (in the case of Piezo1), which has molecular weights of 1.0 kDa for FLAG and 2.8 kDa for 3xFLAG peptide. The dialysis was performed at 4°C against 500 mL of 200 mM KCl, 10 mM HEPES (pH 7.2). The dialysis buffer was replaced in full after 6 hr and again after 12 hr. The dialyzed sample was ultracentrifuged in a TLA rotor to pellet the proteoliposomes at 60,000 × g for 1 hr at 12°C. The proteoliposomes were resuspended in 40 μL of detergent-free buffered solution (200 mM KCl, 10 mM HEPES [pH 7.4]). The proteoliposome sample served as the starting material for subsequent protein reconstitution in droplet lipid bilayers.

Reconstitution of Protein in Droplet Lipid Bilayers

The purified proteins (Piezo1-FLAG WT and mutant E2133A, MscS, and KcsA) were incorporated into droplet lipid bilayers to test their functionality. Droplet lipid bilayers were formed as described previously (Syeda et al., 2008, 2014), with the following modifications. The droplets (~100–200 nL) were dispensed to the tips of two Ag/AgCl electrodes (0.1-mm diameter) in a hexadecane medium. After 5–10 min of incubation, droplets were manipulated to join together. The *cis* droplet contained purified protein (WT-Piezo1, E2133A-Piezo1, MscS, or KcsA) and was connected to the grounded electrode, while the *trans* droplet was connected to the commanding potential electrode so that, at negative applied potentials, cations move from the *cis* to the *trans* side. We actively titrated the proteins in the droplet solution to exclusively get single channels; hence, some of the bilayers were silent and did not evoke channel activity, even in the presence of applied stimulus. It is likely that these bilayers were devoid of any channel protein at the droplet interface. The lipid bilayers were formed between two droplets containing (in mM) 0.5 DPhC liposomes, 500 KCl (200 or 70 KCl, as indicated in the text), 20 HEPES (pH 7.4) in a hexadecane medium. For the formation of asymmetric bilayers, the liposomes contained 90% DPhC + 10% LPA in the *cis* droplet, whereas the symmetric bilayers were made with 100% DPhC in both droplets. We also tested asymmetric bilayers composed of 10% 1-stearoyl-2-hydroxy-sn-glycero-3-PC (LPC) and 90% DPhC in the *cis* droplet but did not achieve stable bilayers to reconstitute and record protein activity (n = 11; data not shown). Additionally, LPA was preferred because of its direct comparison with DOPA's head-group chemistry, as shown previously (Coste et al., 2012). For mannitol gradient experiments, the dried lipids were re-suspended in either 300 mM or 500 mM mannitol, 500 KCl, 10 mM HEPES (pH 7.4). For low-ionic-strength experiments, 500 mM KCl was replaced by 70 mM KCl.

Solvent Injection Assay

The solvent injection experiments were performed by injecting potassium chloride solution (~30 nL) using a nano-injector at the speed of 46 nL/s, as suggested by nano-injector protocols (World Precision Instruments). The nano-injector was steadily brought in contact with the *cis* droplet near the bilayer interface before expelling the volume into the 100-nL droplet. The nano-injector was removed from the bilayer system prior to the electrical recordings. These injection protocols caused a ~30-s disruption in electrical recordings. We also observed that ~70% of the droplets undergo coalescence within 2 min of injection, presumably due to high lytic tension and decreased lipid density in the *cis* monolayer. Nonetheless, the injection assay provides a 30-s to 2-min time frame in which to record reliable channel activity with a sufficient number of events to construct all-point current histograms.

Data Analysis

All the electrical recordings conducted in droplet bilayers were acquired at 10 kHz and online filtered at 2 kHz. Additional offline filtering of 1 kHz was

applied for the purpose of analysis and display. The recordings were performed from at least five different protein purification trials (Figure 1A). Statistical significance was evaluated using an unpaired two-tailed Student's t test for comparing the difference between two samples. Single-channel conductance (γ) was calculated for each experiment by fitting a Gaussian curve to the all-point current histograms. The current amplitudes obtained from the histograms were divided by the applied voltage to calculate γ. The conductance is plotted as mean ± SEM from the indicated number of experiments (n).

SUPPLEMENTAL INFORMATION

Supplemental Information includes Supplemental Experimental Procedures, two figures, and one table and can be found with this article online at http://dx.doi.org/10.1016/j.celrep.2016.10.033.

AUTHOR CONTRIBUTIONS

R.S. and A.P. designed the experiments and wrote the manuscript. R.S., M.N.F., and J.M.K. conducted Piezo1 purification, with help from J.S.S. R.S. conducted electrical recordings and performed analysis. C.D.C. and B.M. provided MscS protein, analyzed bilayer tension data, and wrote the manuscript.

REFERENCES

Anishkin, A., Loukin, S.H., Teng, J., and Kung, C. (2014). Feeling the hidden mechanical forces in lipid bilayer is an original sense. Proc. Natl. Acad. Sci. USA *111*, 7898–7905.

Arnadóttir, J., and Chalfie, M. (2010). Eukaryotic mechanosensitive channels. Annu. Rev. Biophys. *39*, 111–137.

Bass, R.B., Strop, P., Barclay, M., and Rees, D.C. (2002). Crystal structure of Escherichia coli MscS, a voltage-modulated and mechanosensitive channel. Science *298*, 1582–1587.

Battle, A.R., Petrov, E., Pal, P., and Martinac, B. (2009). Rapid and improved reconstitution of bacterial mechanosensitive ion channel proteins MscS and MscL into liposomes using a modified sucrose method. FEBS Lett. *583*, 407–412.

Berrier, C., Pozza, A., de Lacroix de Lavalette, A., Chardonnet, S., Mesneau, A., Jaxel, C., le Maire, M., and Ghazi, A. (2013). The purified mechanosensitive channel TREK-1 is directly sensitive to membrane tension. J. Biol. Chem. *288*, 27307–27314.

Booth, I.R. (2014). Bacterial mechanosensitive channels: progress towards an understanding of their roles in cell physiology. Curr. Opin. Microbiol. *18*, 16–22.

Borbiro, I., Badheka, D., and Rohacs, T. (2015). Activation of TRPV1 channels inhibits mechanosensitive Piezo channel activity by depleting membrane phosphoinositides. Sci. Signal. *8*, ra15.

Brohawn, S.G., Campbell, E.B., and MacKinnon, R. (2014a). Physical mechanism for gating and mechanosensitivity of the human TRAAK K+ channel. Nature *516*, 126–130.

Brohawn, S.G., Su, Z., and MacKinnon, R. (2014b). Mechanosensitivity is mediated directly by the lipid membrane in TRAAK and TREK1 K$^+$ channels. Proc. Natl. Acad. Sci. USA *111*, 3614–3619.

Chalfie, M. (2009). Neurosensory mechanotransduction. Nat. Rev. Mol. Cell Biol. *10*, 44–52.

Corey, D.P., and Hudspeth, A.J. (1979). Response latency of vertebrate hair cells. Biophys. J. *26*, 499–506.

Coste, B., Mathur, J., Schmidt, M., Earley, T.J., Ranade, S., Petrus, M.J., Dubin, A.E., and Patapoutian, A. (2010). Piezo1 and Piezo2 are essential components of distinct mechanically activated cation channels. Science *330*, 55–60.

Coste, B., Xiao, B., Santos, J.S., Syeda, R., Grandl, J., Spencer, K.S., Kim, S.E., Schmidt, M., Mathur, J., Dubin, A.E., et al. (2012). Piezo proteins are pore-forming subunits of mechanically activated channels. Nature *483*, 176–181.

Coste, B., Murthy, S.E., Mathur, J., Schmidt, M., Mechioukhi, Y., Delmas, P., and Patapoutian, A. (2015). Piezo1 ion channel pore properties are dictated by C-terminal region. Nat. Commun. *6*, 7223.

Cox, C.D., Nomura, T., Ziegler, C.S., Campbell, A.K., Wann, K.T., and Martinac, B. (2013). Selectivity mechanism of the mechanosensitive channel MscS revealed by probing channel subconducting states. Nat. Commun. *4*, 2137.

Cox, C.D., Bae, C., Ziegler, L., Hartley, S., Nikolova-Krstevski, V., Rohde, P.R., Ng, C.A., Sachs, F., Gottlieb, P.A., and Martinac, B. (2016). Removal of the mechanoprotective influence of the cytoskeleton reveals PIEZO1 is gated by bilayer tension. Nat. Commun. *7*, 10366.

Dong, Y.Y., Pike, A.C.W., Mackenzie, A., McClenaghan, C., Aryal, P., Dong, L., Quigley, A., Grieben, M., Goubin, S., Mukhopadhyay, S., et al. (2015). K2P channel gating mechanisms revealed by structures of TREK-2 and a complex with Prozac. Science *347*, 1256–1259.

Ge, J., Li, W., Zhao, Q., Li, N., Chen, M., Zhi, P., Li, R., Gao, N., Xiao, B., and Yang, M. (2015). Architecture of the mammalian mechanosensitive Piezo1 channel. Nature *527*, 64–69.

Gillespie, P.G., and Walker, R.G. (2001). Molecular basis of mechanosensory transduction. Nature *413*, 194–202.

Gottlieb, P.A., Bae, C., and Sachs, F. (2012). Gating the mechanical channel Piezo1: a comparison between whole-cell and patch recording. Channels (Austin) *6*, 282–289.

Guharay, F., and Sachs, F. (1984). Stretch-activated single ion channel currents in tissue-cultured embryonic chick skeletal muscle. J. Physiol. *352*, 685–701.

Kung, C. (2005). A possible unifying principle for mechanosensation. Nature *436*, 647–654.

LeMasurier, M., Heginbotham, L., and Miller, C. (2001). KcsA: it's a potassium channel. J. Gen. Physiol. *118*, 303–314.

Lewis, A.H., and Grandl, J. (2015). Mechanical sensitivity of Piezo1 ion channels can be tuned by cellular membrane tension. eLife *4*, e12088.

Martinac, B., Adler, J., and Kung, C. (1990). Mechanosensitive ion channels of E. coli activated by amphipaths. Nature *348*, 261–263.

Martinac, B., Nomura, T., Chi, G., Petrov, E., Rohde, P.R., Battle, A.R., Foo, A., Constantine, M., Rothnagel, R., Carne, S., et al. (2014). Bacterial mechanosensitive channels: models for studying mechanosensory transduction. Antioxid. Redox Signal. *20*, 952–969.

Najem, J.S., Dunlap, M.D., Rowe, I.D., Freeman, E.C., Grant, J.W., Sukharev, S., and Leo, D.J. (2015). Activation of bacterial channel MscL in mechanically stimulated droplet interface bilayers. Sci. Rep. *5*, 13726.

Nilius, B., and Honoré, E. (2012). Sensing pressure with ion channels. Trends Neurosci. *35*, 477–486.

Noël, J., Zimmermann, K., Busserolles, J., Deval, E., Alloui, A., Diochot, S., Guy, N., Borsotto, M., Reeh, P., Eschalier, A., and Lazdunski, M. (2009). The mechano-activated K+ channels TRAAK and TREK-1 control both warm and cold perception. EMBO J. *28*, 1308–1318.

Nomura, T., Cranfield, C.G., Deplazes, E., Owen, D.M., Macmillan, A., Battle, A.R., Constantine, M., Sokabe, M., and Martinac, B. (2012). Differential effects of lipids and lyso-lipids on the mechanosensitivity of the mechanosensitive channels MscL and MscS. Proc. Natl. Acad. Sci. USA *109*, 8770–8775.

Nomura, T., Cox, C.D., Bavi, N., Sokabe, M., and Martinac, B. (2015). Unidirectional incorporation of a bacterial mechanosensitive channel into liposomal membranes. FASEB J. *29*, 4334–4345.

Perozo, E., Cortes, D.M., Sompornpisut, P., Kloda, A., and Martinac, B. (2002). Open channel structure of MscL and the gating mechanism of mechanosensitive channels. Nature *418*, 942–948.

Peyronnet, R., Martins, J.R., Duprat, F., Demolombe, S., Arhatte, M., Jodar, M., Tauc, M., Duranton, C., Paulais, M., Teulon, J., et al. (2013). Piezo1-dependent stretch-activated channels are inhibited by Polycystin-2 in renal tubular epithelial cells. EMBO Rep. *14*, 1143–1148.

Poole, K., Herget, R., Lapatsina, L., Ngo, H.-D., and Lewin, G.R. (2014). Tuning Piezo ion channels to detect molecular-scale movements relevant for fine touch. Nat. Commun. *5*, 3520.

Ranade, S.S., Syeda, R., and Patapoutian, A. (2015). Mechanically activated ion channels. Neuron *87*, 1162–1179.

Retailleau, K., Duprat, F., Arhatte, M., Ranade, S.S., Peyronnet, R., Martins, J.R., Jodar, M., Moro, C., Offermanns, S., Feng, Y., et al. (2015). Piezo1 in smooth muscle cells is involved in hypertension-dependent arterial remodeling. Cell Rep. *13*, 1161–1171.

Ridone, P., Nakayama, Y., Martinac, B., and Battle, A.R. (2015). Patch clamp characterisaton of the effect of cardiolipin on the bacterial mechanosensitive channels of small (MscS) and large (MscL) conductance. Biophys. J. *108*, 561a.

Sukharev, S.I., Blount, P., Martinac, B., Blattner, F.R., and Kung, C. (1994). A large-conductance mechanosensitive channel in E. coli encoded by mscL alone. Nature *368*, 265–268.

Syeda, R., Holden, M.A., Hwang, W.L., and Bayley, H. (2008). Screening blockers against a potassium channel with a droplet interface bilayer array. J. Am. Chem. Soc. *130*, 15543–15548.

Syeda, R., Santos, J.S., and Montal, M. (2014). Lipid bilayer modules as determinants of K$^+$ channel gating. J. Biol. Chem. *289*, 4233–4243.

Syeda, R., Xu, J., Dubin, A.E., Coste, B., Mathur, J., Huynh, T., Matzen, J., Lao, J., Tully, D.C., Engels, I.H., et al. (2015). Chemical activation of the mechanotransduction channel Piezo1. eLife *4*, 1–11.

Syeda, R., Qiu, Z., Dubin, A.E., Murthy, S.E., Florendo, M.N., Mason, D.E., Mathur, J., Cahalan, S.M., Peters, E.C., Montal, M., and Patapoutian, A. (2016). LRRC8 proteins form volume-regulated anion channels that sense ionic strength. Cell *164*, 499–511.

Teng, J., Loukin, S., Anishkin, A., and Kung, C. (2015). The force-from-lipid (FFL) principle of mechanosensitivity, at large and in elements. Pflügers Arch. *467*, 27–37.

Vásquez, V., Cortes, D.M., Furukawa, H., and Perozo, E. (2007). An optimized purification and reconstitution method for the MscS channel: strategies for spectroscopical analysis. Biochemistry *46*, 6766–6773.

Woo, S.H., Lukacs, V., de Nooij, J.C., Zaytseva, D., Criddle, C.R., Francisco, A., Jessell, T.M., Wilkinson, K.A., and Patapoutian, A. (2015). Piezo2 is the principal mechanotransduction channel for proprioception. Nat. Neurosci. *18*, 1756–1762.

Zhang, W., Cheng, L.E., Kittelmann, M., Li, J., Petkovic, M., Cheng, T., Jin, P., Guo, Z., Göpfert, M.C., Jan, L.Y., and Jan, Y.N. (2015). Ankyrin repeats convey force to gate the NOMPC mechanotransduction channel. Cell *162*, 1391–1403.

Supplemental Information

Piezo1 Channels Are Inherently Mechanosensitive

Ruhma Syeda, Maria N. Florendo, Charles D. Cox, Jennifer M. Kefauver, Jose S. Santos, Boris Martinac, and Ardem Patapoutian
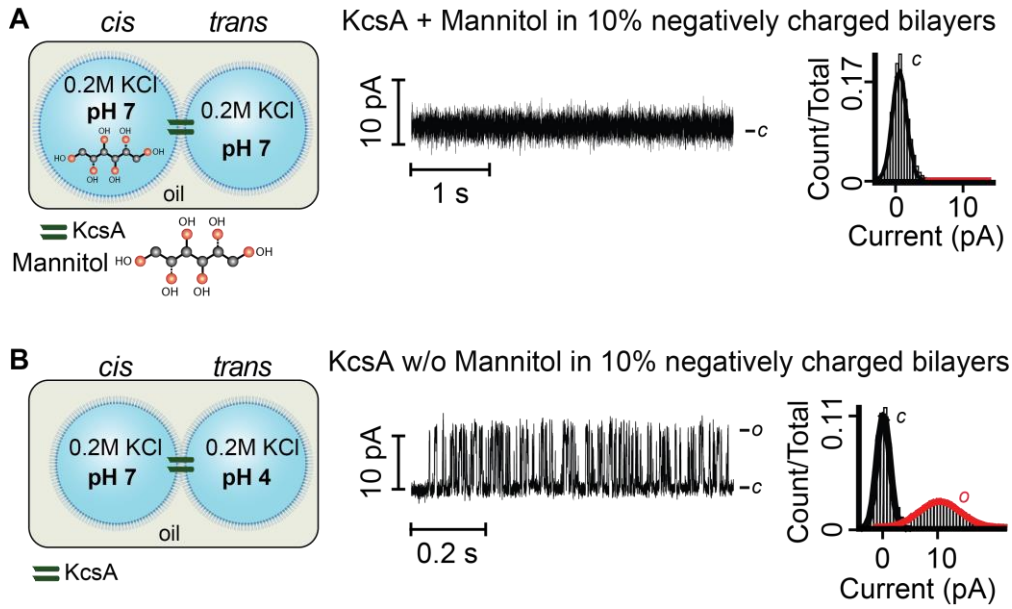
Figure S1

Figure S1: Related to Figure 2. Single-channel recordings of KcsA in 10% negatively charged bilayers. **(A-B)** Experimental illustrations of droplets with and without an osmotic gradient in the presence of 200 mM KCl and indicated pH solutions at V= +100 mV (left panels). Single-channel current recordings (middle panels) and all point current histograms (right panels) for the indicated experimental conditions. The two groups in question i.e. KcsA activity in negatively charged bilayers (10% DOPA + 90% DPhPC) vs. neutral bilayers (100% DPhPC) (Figure 2I and Table S1) are not significantly different as determined by two-tail unpaired *t*-test: P value > 0.05.
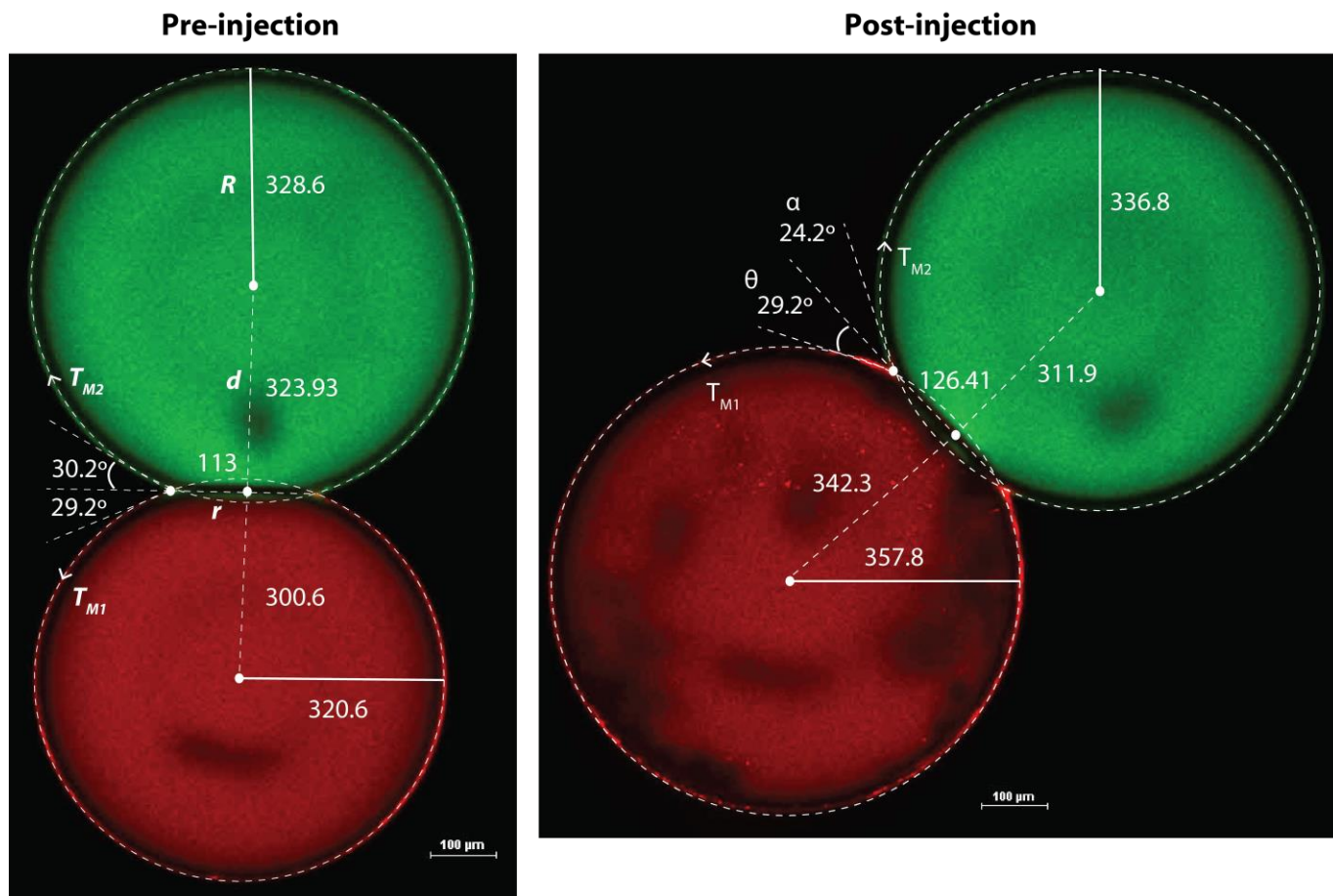
Figure S2: Related to Figure 3. Confocal images of droplet monolayers pre and post-injection. **(A)** Illustration of the measurements taken from two droplets prior to injection. The contact point can be easily delineated and has a radius, r. The green droplet consists of DPhPC and is labeled using 1,2-dioleoyl-*sn*-glycero-3-phosphoethanolamine-N-(carboxyfluorescein). Whereas, the red droplet consists of DPhPC and is labeled using 1,2-dioleoyl-*sn*-glycero-3-phosphoethanolamine-N-(lissamine rhodamine B sulfonyl). **(B)** Demonstration of the expansion in response to the addition of 30 nL to the red droplet. This clearly shows how the angle tangential to the most extreme bilayer contact point changes on expansion and the importance of this in the estimation of tension. The tension in monolayer 1 (T_{M1} - red) is estimated as 3.2 mN/m and the tension in monolayer 2 (T_{M2} - green) is estimated as 0.7 mN/m. All values are shown in μm.

Table S1

Experimental conditions *Cis||trans*	No activity	Single channels	Multiple channels
mPiezo1 in PC||PC (500 mM KCl)	19	0	0
mPiezo1 in LPA||PC (500 mM KCl)	12	6	6
mPiezo1-E2133A in LPA||PC (500 mM KCl)	6	7	5
mPiezo1 in PC||PC (500 mM KCl with mannitol in *cis)*	7	6	4
mPiezo1 in PC||PC (70 mM KCl with mannitol in *cis)*	6	3	4
MscS in PC||PC (200 mM KCl with mannitol in *cis*	2	2	4
mPiezo1 in PC||PC (500 mM KCl with solvent injected in *cis)*	2	2	6
MscS in PC||PC (200 mM KCl with solvent injected in *cis)*	1	1	4
KcsA in PC||PC (200 mM KCl, pH7*cis*, pH7*trans,* solvent injected in cis)	6	0	0
KcsA in PC||PC (200 mM KCl, pH7 *cis*, pH4 *trans*)	2	4	3
KcsA in DOPA||PC (200 mM KCl, pH7 *cis*, pH4 *trans*)	3	3	4
KcsA in PC||PC (200 mM KCl, mannitol in *cis*, pH7 *cis*, pH7 *trans*)	8	0	0

Table S1: Summary of Piezo1, Piezo1-E2133A, MscS and KcsA channel occurrence in droplet lipid-bilayers when tested for the indicated experimental conditions.

Supplemental Experimental Procedures.

Bilayer tension estimates

Here we have estimated the range of tension that could potentially be generated in a symmetrical droplet bilayer system. This tension is generated on addition of a volume of 30 nL to the *cis* droplet. In order to do this we have used the standard equation for calculation of tension due to an area expansion shown below (1):

$$T = K_A \frac{\Delta A}{A} \qquad (1)$$

Where T is the monolayer tension at the contact points between the droplets, K_A is the area expansion modulus of the droplet, ΔA is the change in area of the droplet and A is the initial area of the droplet. In order to calculate the bilayer tension, to which each monolayer contributes separately, we need to calculate the angle tangential to the most extreme bilayer contact point as shown in Figure S2, here termed α and θ. In order to do this we used confocal images of the two monolayer droplets taken before and after injection of the solvent (Figure S2). In this case, using the Young–Dupré equation the total tension in the bilayer can be expressed as;

$$T_b = \cos\theta T_{M1} + \cos\alpha T_{M2} \qquad (2)$$

Equation 2 shows how the tension of each droplet contributes to the bilayer tension where T_b is the bilayer tension, T_{M1} is the tension in monolayer 1 and T_{M2} is the tension in monolayer 2, θ is the angle tangential to the most extreme bilayer contact point of TM1 and α is the angle tangential to the most extreme bilayer contact point of TM2 **(Figure S2).** In order to calculate the expansion of the droplets (ΔA) we use the following equation (3):

$$\Delta A = \frac{A_{M\ new} - A_{M\ initial}}{A_{Minitial}} \qquad (3)$$

Where $A_{Minitial}$ is the initial area of the droplet and A_{Mnew} is the new area of the droplet post injection. As can be seen from the confocal example shown in Figure S2 the droplets are not perfect spheres. We can account for the difference in shape of the droplets using the following equation (4):

$$A = \pi r^2 + [4\pi R^2 - 2\pi r(R - d)] \qquad (4)$$

Where r is the radius of the bilayer contact point, which is a circle, R is the radius of the droplet and d is the distance from the droplet center to the point where the droplets contact – all shown in Figure S2. This results in an average increase in area of 22 ± 3 % (n=4) in the *cis* droplet. If we then assume a K_A of the bilayer at the contact point of 15 mN/m (Bavi et al., 2014) this results in average tension of 2.8 ± 0.7 mN/m in the *cis* monolayer (where volume is injected) and 0.8 ± 0.3 mN/m in monolayer 2. Using larger and thereby stiffer values for the area expansion modulus of DPhPC (~120 mN/m) (Yasmann and Sukharev, 2014) gives rise to values that largely exceed the lytic limit of lipid bilayers (~20 mN/m; Bavi et al., 2014).

Here our estimations suggest that a total bilayer tension in the range of ~ 3.5 mN/m is generated at the bilayer contact point on the addition of 30 nL to the *cis* droplet. Here we assume the boundary between the two droplets i.e. the bilayer, is a perfect circle at the contact point and then calculate its area on expansion. By doing this we obtain a value at the top range of what is possible in the system. The reason this is our upper limit is that it assumes that the expansion simply comes from the lipids in the bilayer stretching and not from new contact forming between the two monolayers, a fact obviously difficult to measure and control. The tension estimates calculated here are in very good agreement with the calculated tension required for half-activation ($P_o = 0.5$) of MscS with a $T_{1/2} = \sim 5.5$ mN/m. These values also begin to give us an idea of the sensitivity of mPiezo1 to membrane tension.

Supplemental References

Bavi, N., Nakayama, Y., Bavi, O., Cox, C.D., Qin, Q.-H., Martinac, B., 2014. Biophysical implications of lipid bilayer rheometry for mechanosensitive channels. Proc. Natl. Acad. Sci. 111, 13864–13869.

Yasmann, A., Sukharev, S., 2014. Properties of Diphytanoyl Phospholipids at the Air–Water Interface. Langmuir 31, 350–357.